Creating vortices in dipolar spinor condensates via rapid adiabatic passage

J.-N. Zhang,[1] L. He,[1] H. Pu,[2] C.-P. Sun,[1] and S. Yi[1]

[1]*Key Laboratory of Frontiers in Theoretical Physics, Institute of Theoretical Physics, Chinese Academy of Sciences, Beijing 100190, China*

[2]*Department of Physics and Astronomy and Rice Quantum Institute, Rice University, Houston, Texas 77251-189-2, USA*

We propose to create vortices in spin-1 condensates via magnetic dipole-dipole interaction. Starting with a polarized condensate prepared under large axial magnetic field, we show that by gradually inverting the field, population transfer among different spin states can be realized in a controlled manner. Under optimal condition, we generate a doubly quantized vortex state containing nearly all atoms in the condensate. The resulting vortex state is a direct manifestation of the dipole-dipole interaction and spin textures in spinor condensates. We also point out that the whole process can be qualitatively described by a simple three-level rapid adiabatic passage model.

I. INTRODUCTION

Ever since the first realization of vortices in an atomic condensate by dynamical phase imprinting [1], quantized vortices in quantum gases have attracted great attention. A variety of techniques have been used to generate vortices, including mechanically stirring the atomic cloud with laser beams [2], rotating asymmetric traps [3], slicing through the condensate with a fast-moving perturbation [4], topological phase imprinting [5], decay of solitons [6], coherently transferring orbital angular momentum from photons to atoms [7], and merging multiply trapped condensates [8]. None of these schemes, however, relies on the specific forms of atom-atom interactions as the vorticity is generated through external perturbation.

In the present work, we propose a scheme to create vortices in a spin-1 condensate by utilizing the magnetic dipole-dipole interaction such that the resulting vortices become a direct manifestation of the underlying dipolar interaction. For convenience, the three spin components of a spin-1 atom are labeled as $\alpha=0$ and ± 1. Starting with a pure condensate of $\alpha=-1$ atoms prepared under an axial magnetic field along negative z axis, we show that a doubly quantized vortex state in $\alpha=1$ component can be created by gradually inverting the magnetic field from negative to positive. With a careful control of the sweeping rate of the magnetic field and other parameters, the efficiency of atom transfer from $\alpha=-1$ to 1 component can approach unity. Quite remarkably, as we will show, this dynamical evolution can be understood as a rapid adiabatic passage process described by a simple three-level Landau-Zener tunneling model.

To put our work in context, we note that, due to their very rich physical properties [9–15], dipolar spinor condensates have become one of the focuses in the study of quantum gases. In the experiment performed by Vengalattore *et al.* [16], evidences suggesting dipolar effects show up in the form of intriguing spin textures whose detection, however, requires sophisticated imaging techniques. Furthermore, whether these spin textures are direct consequences of the dipolar interaction remains a matter of debate as a clear theoretical understanding of these results is still lacking. While

in our scheme, the vortex state is a much more robust signal and can be readily detected via a straightforward density measurement. Detection of the vortex state can be served as an unambiguous evidence of the underlying dipolar interaction. We remark that, in addition to the Rb experiment [16], the effect of dipolar interaction has been experimentally detected in Cr [17], K [18], and Li [19] condensates.

The paper is organized as follows. We describe our model Hamiltonian and its ground-state properties in Sec. II, followed by the direct numerical simulation of the vortex generation dynamics in Sec. III. In Sec. IV, we present a simple Landau-Zener model to explain the dynamics. Discussions of experimental feasibility are presented in Sec. V. Finally, concluding remarks are presented in Sec. VI.

II. MODEL

We consider a condensate of N spin-1 ^{87}Rb atoms. Within the mean-field treatment, the dynamical behavior of the condensate wave functions $\psi_\alpha(\mathbf{r})$ is described by (here and henceforth, summation over repeated indices is assumed)

$$i\hbar\frac{\partial\psi_\alpha}{\partial t} = [T + U + c_0\rho(\mathbf{r})]\psi_\alpha + g\mu_B\mathbf{B}_{\text{eff}}(\mathbf{r})\cdot\mathbf{F}_{\alpha\beta}\psi_\beta, \quad (1)$$

where $T=-\hbar^2\nabla^2/(2m)$, with m being the mass of the atom,

$$U(\mathbf{r}) = \tfrac{1}{2}m\omega_0^2(x^2 + y^2 + \lambda^2 z^2)$$

is the trapping potential, with λ being the trap aspect ratio, $\rho(\mathbf{r})=\psi_\alpha^*\psi_\alpha$ is the total density of the condensate, and $c_0 =4\pi\hbar^2(a_0+2a_2)/(3m)$ characterizes the spin-independent collisional interaction with a_f ($f=0,2$) being the s-wave scattering length in the combined symmetric channel of total spin f. For rubidium atoms, we have $a_0=101.8a_B$ and $a_2 =100.4a_B$, with a_B being the Bohr radius. Furthermore, $g(=-1/2)$ is the Landé g factor, μ_B is the Bohr magneton, and $\mathbf{F}$ is the angular-momentum operator. The effective field includes the external magnetic field $\mathbf{B}=B(t)\mathbf{z}$, and the mean fields originating from the spin-exchange and dipole-dipole interactions
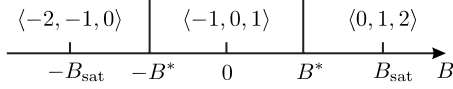
FIG. 1. Schematic plot of the magnetic field dependence of the ground-state structure in an oblate trap.

$$\mathbf{B}_{\text{eff}} = \mathbf{B} + \frac{c_2}{g\mu_B}\mathbf{S}(\mathbf{r}) + \frac{c_d}{g\mu_B}\int d\mathbf{r}' \frac{\mathbf{S}(\mathbf{r}') - 3[\mathbf{S}(\mathbf{r}')\cdot\mathbf{e}]\mathbf{e}}{|\mathbf{r}-\mathbf{r}'|^3},$$
(2)

where $c_2 = 4\pi\hbar^2(a_2-a_0)/(3m)$, $\mathbf{S}(\mathbf{r}) = \psi_\alpha^* \mathbf{F}_{\alpha\beta}\psi_\beta$, $\mathbf{e} = (\mathbf{r}-\mathbf{r}')/|\mathbf{r}-\mathbf{r}'|$, and the strength of dipolar interaction is characterized by $c_d = \mu_0\mu_B^2 g^2/(4\pi)$, with μ_0 being the vacuum magnetic permeability. Note that we have neglected the quadratic Zeeman shift in the equations. For the kind of external magnetic field strength (<1 mG) considered in our work, the quadratic Zeeman energy is completely negligible.

For the numerical results presented in this work, the transverse trapping frequency is taken to be $\omega_0 = (2\pi)100$ Hz. We shall focus on three different trap geometries corresponding to prolate, spherical, and oblate trapping potentials with, respectively, $\lambda = 0.25$, 1, and 6. Unless otherwise stated, the total number of atoms is chosen to be $N = 2\times 10^6$.

Let us first recall the ground-state structure in magnetic field. For convenience, we assume that the magnetic field is along the negative z axis, i.e., $B < 0$. In an oblate trap, as shown in Ref. [12], the ground-state wave function takes the form $\psi_\alpha(\mathbf{r}) = \sqrt{\rho_\alpha(\mathbf{r})}\exp[i(w_\alpha\varphi + \varphi_\alpha)]$, where the densities $\rho_\alpha = |\psi_\alpha|^2$ are axially symmetric, w_α are the winding numbers, φ is the azimuthal angle, and φ_α are phase angles satisfying $2\varphi_0 - \varphi_1 - \varphi_{-1} = 0$. There exists a critical magnetic field strength B^* such that $\langle w_1, w_0, w_{-1}\rangle = \langle -1, 0, 1\rangle$ and $\langle -2, -1, 0\rangle$ for $0 > B > -B^*$ and $B < -B^*$, respectively. Across the critical field $-B^*$, the total energy is continuous, indicating a second-order phase transition. Obviously, for sufficiently strong magnetic field, the system will be polarized. We can define the saturation field strength $B_{\text{sat}} > 0$ such that when $B < -B_{\text{sat}}$, over 99.9% of the population will be in $\alpha = -1$ component. The saturation field is an increasing function of N and λ. For parameters adopted in this paper, B_{sat} is about several tens of micro-Gauss. Finally, incorporating the results corresponding to $B > 0$ case gives us the complete picture of ground-state phases in an oblate trap, schematically plotted in Fig. 1.

In a spherical trap, the axial symmetry of the densities ρ_α is lost under weak magnetic field. However, if one increases the magnetic field strength, ρ_α recover axial symmetry, especially when the system becomes polarized. The saturation field in a spherical trap is only about several micro-Gauss, much lower than that in an oblate trap. Finally, only polarized phase exists in a prolate trap.

III. DYNAMICAL SIMULATION

To study the dynamic properties, we numerically evolve Eq. (1) with the initial wave functions being the ground state under field $B_0 < -B_{\text{sat}}$. The magnetic field is assumed to vary linearly as
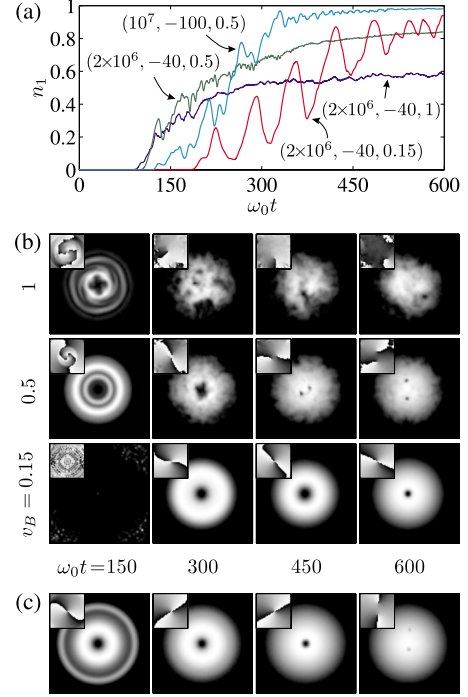

FIG. 2. (Color online) Typical dynamic behaviors in an oblate trap ($\lambda = 6$). (a) The time dependence of reduced atom number n_1 for various control parameters (N, B_0, v_B). (b) The integrated densities $\bar{\rho}_1(x,y)$ and phases (insets) of wave function $\psi_1(x,y,0)$ for $(N,B_0) = (2\times 10^6, -40)$ with various v_B's. (c) Same as (b) except for $N = 10^7$, $B_0 = -100$ μG, and $v_B = 0.5$.

$$B(t) = B_0 + v_B t,$$

where $v_B > 0$ (in units of $\mu G\times\omega_0$) is the sweeping rate of the magnetic field. We shall explore how to control the dynamic behaviors of rubidium condensates by tuning parameters λ, N, B_0, and v_B.

In Fig. 2(a), we plot the time dependence of the reduced atom number $n_\alpha = N^{-1}\int d\mathbf{r}\rho_\alpha(\mathbf{r})$ for $\alpha = 1$ spin component in an oblate trap. Since n_1 is essentially zero at the beginning, its final value can be regarded as a measure of the atom transfer efficiency. n_1 remains negligible until B is close to zero. It then grows with oscillations and eventually reaches some steady-state value. Given N and B_0, the asymptotic transfer efficiency increases as one lowers the sweeping rate and it can be as high as 80% for $N = 2\times 10^6$ and $v_B = 0.15$. However the onset of population transfer occurs earlier for larger v_B. As we shall show below, the relation between n_1 and v_B can be understood using a simple Landau-Zener tunneling (LZT) model of a three-level system.

Figure 2(b) shows the time dependence of integrated density

$$\bar{\rho}_\alpha(x,y) = \int dz\rho_\alpha(\mathbf{r}).$$

We see that the density depletion appears at the center of the condensate ψ_1. Further examination of the phases of the wave function confirms that it is a doubly quantized vortex which is unstable against splitting into two singly quantized
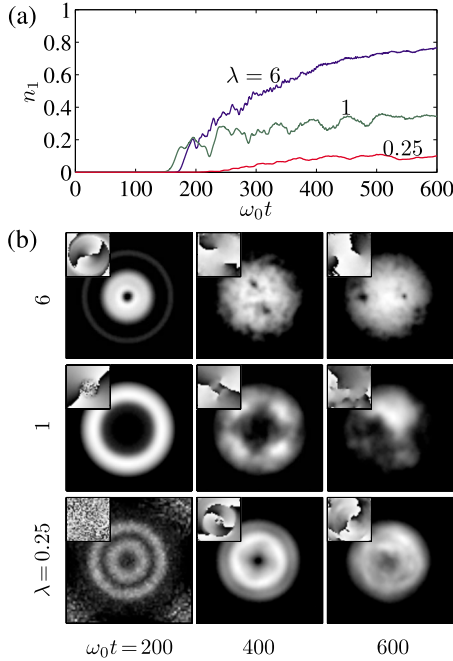
FIG. 3. (Color online) Time dependence of relative population (a) n_1 and integrated density (b) $\bar{\rho}_1$ in various trapping potentials for $B_0 = -60$ μG and $v_B = 0.5$. Insets in (b) show the phases of wave function $\psi_1(x, y, 0)$.

vortices [20]. Indeed one can see that, as the system continues to evolve, the dynamical instability of the wave function ψ_1 sets in and the doubly quantized vortex breaks into two vortices. The time that this break happens is sensitive to the magnetic field sweeping rate: it happens at a later time for a lower sweeping rate (i.e., smaller v_B).

In Fig. 2(c), we show the evolution of the integrated density $\bar{\rho}_1$ for an increased total number of atoms $N = 10^7$. In this case, the atom transfer efficiency becomes nearly unity [see Fig. 2(a)] even for a rather large sweeping rate $v_B = 0.5$ and a stronger initial magnetic field $B_0 = -100$ μG. The doubly quantized vortex state survives for a much longer time compared to the previous case with smaller N but the same sweeping rate.

The creation of the doubly quantized vortex can be most easily understood by noting that the dipolar interaction conserves the total angular momentum $\mathbf{J} = \mathbf{F} + \mathbf{L}$. When an axial magnetic field is present, J_z is still conserved. For the initial condensate under study, we have $m_J = m_F = -1$. If we assume that all atoms are transferred to $\alpha = 1$ state at the end of the process, the spin angular momentum then becomes $m_F = 1$. As a result, wave function ψ_1 must carry an orbital angular momentum $m_L = -2$ [21], representing a doubly quantized vortex, in order to conserve J_z. By stark contrast, in the absence of the dipolar interaction, F_z and L_z will be individually conserved. In our case, all the population would remain in the initial spin state $\alpha = -1$. Therefore, the population dynamics and the generation of the vorticity both serve as unambiguous evidence of the underlying dipolar interaction.

Next, we turn to study the effects of trap geometry on the population transfer and the wave functions. In Fig. 3, we present the simulation results for all three trap geometries
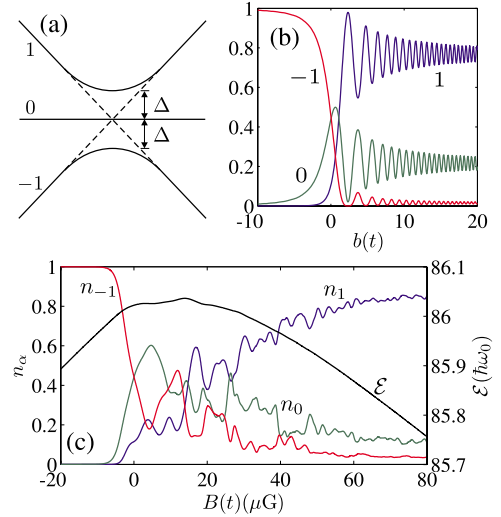

FIG. 4. (Color online) (a) Eigenenergies of H_{LZT} as a function of axial field b. (b) Population dynamics of the LZT model with $b_x = 1$, $b_0 = -10$, and $v_b = 1.5$. (c) Reduced atom numbers n_α and total energy per atom $\mathcal{E}$ versus magnetic field in an oblate trap ($\lambda = 6$), obtained from the full numerical simulation of Eq. (1). Other parameters are $B_0 = -40$ μG and $v_B = 0.25$.

with $B_0 = -60$ μG and $v_B = 0.5$. Clearly, for given B_0 and v_B, n_1 increases with trap aspect ratio λ. From the plots of the density profile in Fig. 3(b), it can be seen that the doubly quantized vortex in a prolate trap is most stable against splitting. In such prolate trap, the population transfer efficiency is low. The vortex core is filled by a large number of spin $\alpha = -1$ atoms, which provides an effective pinning effect that helps to stabilize the vortex state [22]. However, in both prolate and spherical traps, the vortices suffer a different kind of instability: the vortex line tends to be distorted and cannot remain straight along the axial direction. A consequence of such instability is to reduce the contrast of the vortex core in the integrated density profile $\bar{\rho}(x, y)$. From these results, we conclude that an oblate trap provides the best candidate to study this phenomenon.

IV. LANDAU-ZENER MODEL

To gain more insights into the population dynamics of the system, let us consider the spin dynamics of a single spin-1 particle under external magnetic field. For the simplest case, it reduces to the model Hamiltonian

$$H_{\text{LZT}} = b(t)F_z + b_x F_x, \qquad (3)$$

where, without loss of generality, the transverse field b_x is assumed to be a constant and along the x axis. Here all quantities are taken to be dimensionless. The energy spectrum of H_{LZT} is schematically plotted in Fig. 4(a) as a function of the axial magnetic field strength b. The presence of b_x changes the three-level crossing at $b = 0$ into anticrossings. The minimum gap between two eigenvalues of H_{LZT} is $\Delta = \sqrt{2} b_x$. Equation (3) describes essentially the LZT of three levels [23]. Figure 4(b) illustrates an example of the dynamics according to the LZT model. Under a large initial axial field

$b_0 < 0$, the atom is prepared in $\alpha = -1$ state. As we sweep the axial field linearly, $b(t) = b_0 + v_b t$, over the anticrossings, $\alpha = 0$ state is first populated, followed by $\alpha = 1$ state. Namely, the wave function bifurcates into the states forming the anticrossing and thus becomes a coherent superposition of different spin states. This coherent superposition is the cause for the population oscillations which are suppressed at large t limit. The asymptotical transition probability to $\alpha = 1$ state is [23]

$$p_1 = (1 - e^{-\pi b_x^2 / v_b})^2, \tag{4}$$

an increasing function of b_x while a decreasing one of v_b. Moreover, the population oscillations disappear completely for sufficiently small sweeping rate v_b as the adiabatic limit is reached, realizing a rapid adiabatic passage process which represents an important method of transferring population from one quantum state to another.

In Fig. 4(c), we present the B dependence of the reduced atom number n_α in a dipolar spinor condensate. Here the transverse field, $\mathbf{B}_{\text{eff}}^{\perp}$, is the transverse component of the effective field [Eq. (2)]. Consequently, it has nontrivial spatial and temporal dependences. Despite the complexity of the condensate system, we still see a remarkable qualitative agreement between the full model and the LZT model: the latter captures all the essential features of the condensate population dynamics. In Fig. 4(c), we also plot the total energy per atom $\mathcal{E}$ as a function of B. Again we see that this curve agrees qualitatively with the lowest adiabatic energy level in the LZT model as shown in Fig. 4(a).

The transition probability Eq. (4) can also be used to interpret the trap geometry dependence of population transfer efficiency n_1. Even through $|c_2|$ is about ten times larger than c_d for rubidium atom, we find in our simulation that the contribution to $\mathbf{B}_{\text{eff}}^{\perp}$ [see Eq. (2)] is mainly provided by the dipole-dipole interaction and is enhanced by the oblate geometry. Furthermore, the dipolar interaction can also be enhanced by increasing the total number of atoms N, which explains the atom number dependence of the transfer efficiency n_1.

V. DISCUSSION

In this section, let us discuss the experimental feasibility of our proposed scheme. For the parameters used in our full numerical simulations, we always see oscillations in the population dynamics, meaning that we have not reached the complete adiabatic limit in our full simulation. In any case, it is not necessary to reach the complete adiabatic limit to demonstrate the effects studied here. In practice, the lifetime of the condensate (typically on the order of seconds) may also set a constraint on whether adiabatic limit can be reached. In our simulation, we always limit the total time to be below 1 s. However, this time scale can be further shortened by choosing a larger trapping frequency ω_0. For instance, if we increase the ω_0 by a factor of 8 as in Ref. [13], the saturation magnetic field can be as high as milli-Gauss. As a consequence, the ramp time can be shortened to around tenth of second.
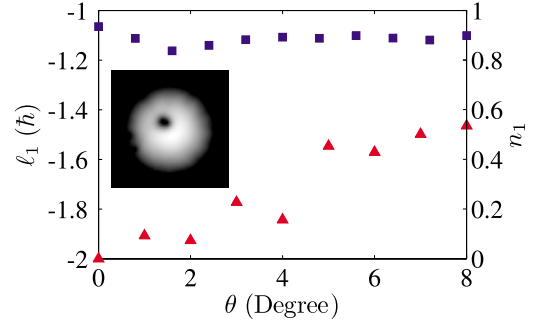

FIG. 5. (Color online) The θ dependence of ℓ_1 (red triangles) and n_1 (blue squares) at time $\omega_0 t = 600$. Other parameters are $\lambda = 6$, $B_0 = -40 \ \mu G$, and $v_B = 0.15$. Inset shows the integrated density $\bar{\rho}_1$ at $\omega_0 t = 600$ for $\theta = 3°$.

In our discussion, we have always assumed that the external magnetic field is perfectly aligned along the trap symmetry axis, the z axis. A natural question to ask is: What happens if the field deviates from the z axis by a small angle due to misalignment? To address this problem, we run our full numerical simulations with the magnetic field tilted by an angle θ with respect to z axis. The tilted magnetic field results in an external uniform transverse field which, based on the Landau-Zener model, also induces the population transfer, but no vortex generation, to $\alpha = 1$ spin state. In Fig. 5, we present results for the tilting angle dependence of n_1 and the orbital angular momentum per atom in $\alpha = 1$ spin component, ℓ_1. As one can see, n_1 only slightly depends on θ; the absolute value of ℓ_1 is, however, lowered as one increases θ since those transferred atoms due to the external transverse field do not carry orbital angular momentum. We point out that the nonmonotonicity of $\ell_1(\theta)$ is due to the large population oscillation for the chosen parameters. Consequently, as shown in the inset of Fig. 5, the vortex core moves away from the center of the trap. These results demonstrate that our proposed scheme is rather robust against magnetic field misalignment: a tilted field will produce an off-centered vortex, but the main features of the proposal remain unchanged as long as the tilting angle is reasonably small.

Finally, we remark that in previous studies on the Einstein–de Haas effect of dipolar spinor condensates, the magnetic field is usually inverted suddenly [13–15]. While in this work, the inverting process of the magnetic field is controlled deliberately, such that we may take advantage of the LZT to realize much higher population transfer efficiency and better control of the system.

VI. CONCLUSION

In conclusion, we have studied the dynamics of a rubidium spinor condensate under a time-dependent axial field. We show that by sweeping the magnetic field and inverting its direction, a doubly quantized vortex containing nearly all atoms in the condensates is created. We have shown that this scheme is robust against small misalignment of the magnetic field. Despite of the complicated nature of the full system, the population dynamics discussed here can be understood as

a rapid adiabatic passage process described by a simple three-level Landau-Zener tunneling model. Since our scheme critically depends on the properties of the dipolar interaction, not only does it provide a method for generating vortices in atomic condensates, it can also be used as a simple and robust mechanism for the experimental demonstration of dipolar effects in spinor condensates. We hope our work will stimulate experimental efforts along this line.

[1] M. R. Matthews, B. P. Anderson, P. C. Haljan, D. S. Hall, C. E. Wieman, and E. A. Cornell, Phys. Rev. Lett. **83**, 2498 (1999).

[2] K. W. Madison, F. Chevy, W. Wohlleben, and J. Dalibard, Phys. Rev. Lett. **84**, 806 (2000).

[3] E. Hodby, G. Hechenblaikner, S. A. Hopkins, O. M. Maragò, and C. J. Foot, Phys. Rev. Lett. **88**, 010405 (2001).

[4] J. R. Abo-Shaeer, C. Raman, J. M. Vogels, and W. Ketterle, Science **292**, 476 (2001); P. C. Haljan, I. Coddington, P. Engels, and E. A. Cornell, Phys. Rev. Lett. **87**, 210403 (2001); S. Inouye, S. Gupta, T. Rosenband, A. P. Chikkatur, A. Görlitz, T. L. Gustavson, A. E. Leanhardt, D. E. Pritchard, and W. Ketterle, *ibid.* **87**, 080402 (2001).

[5] T. Isoshima, M. Nakahara, T. Ohmi, and K. Machida, Phys. Rev. A **61**, 063610 (2000); A. E. Leanhardt, A. Görlitz, A. P. Chikkatur, D. Kielpinski, Y. Shin, D. E. Pritchard, and W. Ketterle, Phys. Rev. Lett. **89**, 190403 (2002); A. E. Leanhardt, Y. Shin, D. Kielpinski, D. E. Pritchard, and W. Ketterle, *ibid.* **90**, 140403 (2003).

[6] Z. Dutton, M. Budde, C. Slowe, and L. V. Hau, Science **293**, 663 (2001); B. P. Anderson, P. C. Haljan, C. A. Regal, D. L. Feder, L. A. Collins, C. W. Clark, and E. A. Cornell, Phys. Rev. Lett. **86**, 2926 (2001).

[7] M. F. Andersen, C. Ryu, P. Cladé, V. Natarajan, A. Vaziri, K. Helmerson, and W. D. Phillips, Phys. Rev. Lett. **97**, 170406 (2006); K. C. Wright, L. S. Leslie, A. Hansen, and N. P. Bigelow, *ibid.* **102**, 030405 (2009).

[8] D. R. Scherer, C. N. Weiler, T. W. Neely, and B. P. Anderson, Phys. Rev. Lett. **98**, 110402 (2007).

[9] S. Yi and H. Pu, Phys. Rev. Lett. **97**, 020401 (2006).

[10] Y. Kawaguchi, H. Saito, and M. Ueda, Phys. Rev. Lett. **97**, 130404 (2006).

[11] M. Takahashi, S. Ghosh, T. Mizushima, and K. Machida, Phys. Rev. Lett. **98**, 260403 (2007).

[12] S. Yi and H. Pu, e-print arXiv:0804.0191.

[13] Y. Kawaguchi, H. Saito, and M. Ueda, Phys. Rev. Lett. **96**, 080405 (2006).

[14] L. Santos and T. Pfau, Phys. Rev. Lett. **96**, 190404 (2006).

[15] K. Gawryluk, M. Brewczyk, K. Bongs, and M. Gajda, Phys. Rev. Lett. **99**, 130401 (2007).

[16] M. Vengalattore, S. R. Leslie, J. Guzman, and D. M. Stamper-Kurn, Phys. Rev. Lett. **100**, 170403 (2008).

[17] J. Stuhler, A. Griesmaier, T. Koch, M. Fattori, T. Pfau, S. Giovanazzi, P. Pedri, and L. Santos, Phys. Rev. Lett. **95**, 150406 (2005).

[18] M. Fattori, G. Roati, B. Deissler, C. D'Errico, M. Zaccanti, M. Jona-Lasinio, L. Santos, M. Inguscio, and G. Modugno, Phys. Rev. Lett. **101**, 190405 (2008).

[19] S. E. Pollack, D. Dries, M. Junker, Y. P. Chen, T. A. Corcovilos, and R. G. Hulet, Phys. Rev. Lett. **102**, 090402 (2009).

[20] H. Pu, C. K. Law, J. H. Eberly, and N. P. Bigelow, Phys. Rev. A **59**, 1533 (1999); K. Gawryluk, M. Brewczyk, and K. Rzażewski, J. Phys. B **39**, L225 (2006); Y. Shin, M. Saba, M. Vengalattore, T. A. Pasquini, C. Sanner, A. E. Leanhardt, M. Prentiss, D. E. Pritchard, and W. Ketterle, Phys. Rev. Lett. **93**, 160406 (2004).

[21] P. Zhang, H. H. Jen, C. P. Sun, and L. You, Phys. Rev. Lett. **98**, 030403 (2007).

[22] J. A. M. Huhtamäki, M. Möttönen, and S. M. M. Virtanen, Phys. Rev. A **74**, 063619 (2006).

[23] C. E. Carroll and F. T. Hioe, J. Phys. A **19**, 2061 (1986).